

can proceed even though the winter chilling requirement (winter rest) of a tree has not been completed fully.

Evidence from grafting experiments and chemical treatments to break winter rest, and studies of genetic variability indicate that the processes and phenomena of dormancy are at least partially independent of each other. Different buds and branches and other parts of the same plant may initiate dormancy, break dormancy, and renew vegetative growth independently.

Initiation and cessation of dormancy can be triggered by a number of environmental variables: photoperiod, temperature, nutrition, water, an array of chemicals, and shock treatments. Dormancy regulation must either involve a variety of receptors or involve receptors that are responsive to a variety of stimuli. Unless dormancy is defined in a highly restricted sense (that is, possession of chilling requirement), it is hard to conceive of a single receptor or regulator that controls all of the phenomena of dormancy. A large number of genes are definitely involved and hence a large number of enzymes. The kinds of enzymes, their numbers, and their concentrations can be regulated by manipulating the environment.

References and Notes

1. A. W. Galston and P. J. Davies, *Science* **163**, 1288 (1969).
2. J. Levitt, in *Hardiness in Plants*, J. Levitt, Ed. (Academic Press, New York, 1956).
3. T. T. Kozlowski, *Bot. Rev.* **30**, 334 (1964).
4. J. Romberger, *U.S. Dep. Agr. Tech. Bull. No. 123* (1963).
5. I. M. Vasil'yev, *Wintering of Plants* (American Institute of Biological Sciences, Washington, D.C., 1961).
6. A. Vegis, *Annu. Rev. Plant Physiol.* **15**, 185 (1964).
7. P. F. Wareing, C. F. Eagles, P. M. Robinson, in *Colloq. Intern. No. 123 Centr. Nat. Rech. Sci., Paris* (1964), pp. 377-386.
8. G. T. Jones, thesis, Univ. of Chicago (1938).
9. W. H. Chandler, in *Deciduous Orchards* (Lea & Febiger, Philadelphia, ed. 2, 1951), p. 40.
10. P. P. Larson, in *Tree Growth*, T. T. Kozlowski, Ed. (Ronald Press, New York, 1962), pp. 97-117.
11. C. M. Stewart, *Tappi* **40**, 244 (1957).
12. H. A. Borthwick and S. A. Hendricks, *Science* **132**, 1223 (1960).
13. P. F. Wareing, *Annu. Rev. Plant Physiol.* **7**, 191 (1956).
14. A. Vegis, *Symb. Bot. Upsal.* **14**, 1 (1955).
15. T. O. Perry, *Plant Physiol.* **43** (11), 1866 (1968).
16. E. B. Matzke, *Amer. J. Bot.* **23**, 446 (1936).
17. P. F. Wareing, *Physiol. Plant.* **7**, 261 (1954).
18. T. T. Kozlowski and T. A. Peterson, *Bot. Gaz.* **124**, 146 (1962).
19. T. D. Rudolph, *Forest Sci. Monogr. No. 6* (1964); R. Zahner, J. E. Lotan, W. D. Baughman, *Forest Sci.* **10**, 361 (1964).
20. M. Büsgen and E. Münsch, in *The Structure and Life in Forest Trees*, translated by T. Thomson (Wiley, New York, ed. 3, 1931), p. 104.
21. T. O. Perry, *Forest Sci.* **8**, 336 (1962).
22. R. M. Irving and F. O. Lanphear, *Plant Physiol.* **42**, 1191 (1967).
23. T. O. Perry and Chi Wu Wang, *Ecology* **41**, 785 (1960).
24. F. E. Denny and E. N. Stanton, *Proc. Amer. Soc. Hort. Sci.* **77**, 107 (1928).
25. K. Ladefoged, *Kgl. Danske Videnskab. Selskab. Biol. Skr.* **7** (3), 1 (1952).
26. P. F. Wareing, *Physiol. Plant.* **4**, 546 (1951).
27. J. E. Lodewick, *N.Y. State Coll. Forest. Syracuse Univ. Tech. Publ. No. 23* (1928).
28. T. O. Perry and W. R. Simons, *Forest Sci.* **13** (4), 400 (1967).
29. F. V. Coville, *J. Agr. Res.* **20**, 151 (1920); G. Klebs, *Bot. Zentralbl.* **119**, 426 (1912); J. Parker, *Protoplasma* **48**, 147 (1957); T. O. Perry, *J. Forest.*, in press.
30. W. Tranquillini, *Mitt. Forstl. Bund. Maria-brunn* **60**, 501 (1963).
31. L. C. Pearson and D. B. Lawrence, *Amer. J. Bot.* **45**, 383 (1958).
32. S. B. Hendricks and H. W. Siegelman, in *Comprehensive Biochemistry*, M. Florkin and E. S. Stotz, Eds. (Elsevier, Amsterdam, 1967), vol. 27, pp. 211-235.
33. T. Hemberg, *Physiol. Plant.* **2**, 37 (1949); C. H. Hendershott and D. R. Walker, *Amer. Soc. Hort. Sci.* **74**, 121 (1959).
34. R. Zahner, personal communication.
35. E. Ball, *Growth* **24**, 91 (1960).
36. J. A. Romberger, R. J. Varnell, C. A. Tabor, *U.S. Dep. Agr. Tech. Bull. No. 1409* (1970).
37. W. L. Howard, *Univ. Mo. Agr. Exp. Sta. Bull. No. 1* (1910), p. 101.
38. H. Smith and N. P. Kefford, *Amer. J. Bot.* **59**, 1002 (1964).
39. P. F. Wareing, in *Trends in Plant Morphogenesis*, E. G. Cutter, Ed. (Longmans, Green & Co., London, 1966).
40. J. W. Cornforth, B. V. Milborrow, G. Ryback, P. F. Wareing, *Nature* **205**, 1269 (1965); C. F. Eagles and P. F. Wareing, *Physiol. Plant.* **17**, 697 (1964).
41. G. V. Hoad, *Life Sci.* **6**, 1113 (1967).
42. L. N. Lewis and J. C. Bakhshi, *Plant Physiol.* **43** (3), 359 (1968).
43. A. E. DeMaggio, and J. A. Freeberg, *Can. J. Bot.* **47**, 1165 (1969).
44. R. M. Irving and F. O. Lanphear, *Plant Physiol.* **43**, 9 (1968).
45. G. H. Lamb, *Mon. Weather Rev. Suppl. II* (1915).
46. H. B. Kriebel, in *Proc. Soc. Amer. Forest.* (Memphis, Tennessee, 1956), pp. 79-82; J. S. Olsen and H. Nienstaedt, *Science* **125**, 492 (1957); H. Iregens-Moller, *Forest Sci.* **4**, 325 (1958); S. S. Pauley and T. O. Perry, *J. Arnold Arboretum* **35**, 167 (1954).
47. J. E. Varner and G. R. Chandra, *Proc. Nat. Acad. Sci. U.S.A.* **52**, 100 (1964).
48. Supported in part by NSF grant GB 7153.

Magnetic Resonances and Waves in Simple Metals

Transparencies of alkali metals near cyclotron and spin resonances reveal many-body interactions.

W. M. Walsh, Jr.

The high reflectivity of smooth metal surfaces is among their most familiar physical properties. At room temperature, electromagnetic radiation is efficiently reflected at all frequencies below the ultraviolet region. Since this screening or skin-effect phenomenon results directly from the metal's large electrical conductivity, it is somewhat of a paradox that purification and cool-

ing to liquid helium temperatures both greatly increase the direct current (d-c) conductivity and yet create "windows" or regions of partial transparency in the audio, radio, and microwave frequency ranges. In fact the windows are magnetotransparencies which require the presence of strong magnetic fields to curl the conduction-electron trajectories into cyclotron orbits. These

changes in trajectory seriously modify the screening characteristics of the conduction electrons.

The ability of ionized gases or fluids (plasmas) to support a variety of harmonic disturbances (waves) and to transmit them many wavelengths is well known (1). The study of such phenomena in semiconductors, semimetals, and metals—solid-state plasma physics—has become an active branch, during the past decade, of the investigation of the electronic properties of solids (2). Research activity has been particularly fruitful in the case of the simplest metals—the light alkali metals sodium and potassium—in which the greatest variety of wave propagation phenomena has been observed; also the nearly total absence of band-structure complexities in these metals greatly facilitates comparison of theory and experiment. In this article the various plasma and spin-wave excitations thus far discovered in the alkali metals are

The author is head of the Solid State and Physics of Metals Research Department of the Bell Telephone Laboratories, Murray Hill, New Jersey 07974.

qualitatively reviewed with emphasis on the specific information which these rather novel experiments have provided about the collective behavior of conduction electrons.

Certain of these wave excitations are closely associated with magnetic resonances in both the orbital and spin degrees of freedom and are explicitly sensitive to many-body interactions (correlation and exchange). Such collective forces are usually accounted for in rather ad hoc fashion in normal metals where, in most circumstances, the conduction electrons behave as independent particles subject to the Pauli exclusion principle. Certain plasma waves, however, probe the metal in a more revealing fashion than do most other phenomena. Their quantitative explanation requires a description in which the electronic interactions are more precisely taken into account via the Landau theory of Fermi liquids. In an effort to introduce such complications gradually, the various waves are presented in order of increasing sophistication instead of the historical order of their discovery.

Simple Metals

The basic premise of the band theory of metals is that each delocalized valence electron, one per atom in the case of the alkali metals, may be thought of as an independent particle-wave entity with electric charge e , crystal momentum \mathbf{p} , and spin angular momentum \mathbf{S} . The periodic lattice potential felt by an individual conduction electron is due to the essentially static positive-ion cores, which are screened by all the other mobile electrons. The resultant set of allowed single-particle energy states constitutes the conduction band. The states are filled according to Fermi-Dirac statistics to satisfy the exclusion principle requirement that each state be occupied by at most two electrons of antiparallel spin. Even at the absolute zero of temperature the states are filled up to an energy $E_F \sim 3$ electron volts, which defines the Fermi surface in crystal momentum space (see Fig. 1). Although in most metals the Fermi surface is quite complicated, in sodium and potassium the screened lattice potential is so smooth that their Fermi surfaces are almost exactly spherical and correspond to the isotropic parabolic energy band $E = p^2/2m$ of Fig. 1. The band mass, m , differs very little from the free-electron

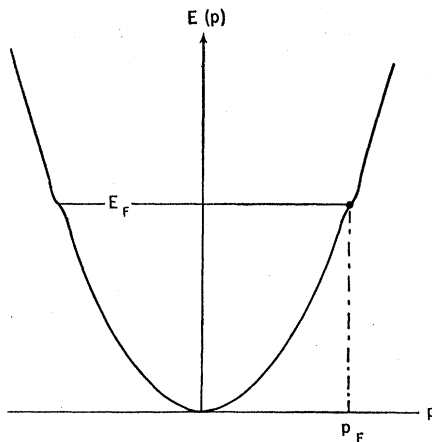


Fig. 1. The simple parabolic conduction band of a nearly-free-electron metal ($E = p^2/2m$) filled to the Fermi energy E_F . The map of p_F in three dimensions is a spherical Fermi surface. The slight distortion of $E(p)$ near E_F corresponds to many-body enhancement of the conduction-electron effective mass.

value m_0 , because of the smoothness of the screened lattice potential.

However, electrons at the Fermi energy, which are the only ones free to participate in low energy electric and magnetic phenomena, are also free to interact with each other and with the ionic lattice in ways not properly accounted for in the band description. Correlations in their motions due to the short-range part of their Coulomb interaction (electron-electron coupling) as well as polaron-like local deformation of the ionic lattice (electron-phonon coupling) cause these observable conduction electrons to have an effective mass m^* significantly greater than m_0 . (This difference is schematically indicated as a band distortion at the Fermi energy in Fig. 1.) In sodium and potassium the ratio m^*/m_0 is 1.24 and 1.21, respectively. The velocity of these electrons, $v_F = p_F/m^* \sim 10^8$ centimeters per second, is correspondingly reduced because the Fermi momentum p_F is an overall band property and is not affected by the short range couplings between electrons on the Fermi surface.

Similarly χ , the temperature-independent paramagnetic susceptibility of the electrons at the Fermi energy, is also appreciably larger than its free-electron value χ_0 . The enhancement of the susceptibility is even greater than the enhancement of the effective mass and is caused by spin-dependent exchange forces also not accounted for in the purely statistical treatment.

To the extent that the increases in

m^* and χ over their free-electron values are considered to be weak corrections (renormalizations) of the band description these modified electrons (quasiparticles) may still be treated as statistically independent entities. The mass and susceptibility enhancements will therefore be called *implicit* many-body effects, reserving the label *explicit* for higher-order interaction effects which go beyond the spirit of the nearly-free-electron description. The explicit many-body effects do not appreciably influence most properties of metals so the experimental demonstration of their reality is one of the most interesting accomplishments of solid-state plasma physics.

Wave Propagation and Reflection

A plane electromagnetic wave traveling in vacuum oscillates in time t and distance x as $\exp i(\omega t - k_0 x)$ where $\omega = 2\pi f$ is the angular frequency in radians per second (f is the frequency in hertz) and $k_0 = 2\pi/\lambda_0$ is the wave number in reciprocal centimeters (λ_0 is the wavelength in centimeters). The phase velocity $v_\phi = f\lambda_0 = \omega/k_0$ is the invariant speed of light $v_\phi = c = 3 \times 10^{10}$ centimeters per second. The wave number is entirely real because there is no damping. When the wave is normally incident on the flat surface of a medium with a dielectric constant ϵ part of the energy is reflected and the transmitted component propagates more slowly with the wave number

$$k = k_0 (\epsilon)^{1/2} \quad (1)$$

If the medium is a good insulator ϵ and, therefore, k are real so the penetrating wave component continues to travel without damping.

If the medium is in the form of a plane-parallel slab the penetrating wave will be partially internally reflected at the second surface and partially transmitted. Standing-wave resonances of the internally reflected component will occur if the slab thickness L is equal to an integral number of half-wavelengths ($kL = n\pi$, where n is an integer). By varying the frequency a set of transmission peaks (reflection dips) may be observed which reveal any frequency dependence (dispersion) of the dielectric constant. This basic experimental technique (Fabry-Perot resonance) carries over into the world of metals with many differences of detail.

The total dielectric "constant" of a medium having a finite electrical con-

ductivity σ is the sum of contributions from the immobile constituents ϵ_l and from conduction currents

$$\epsilon = \epsilon_l + \frac{4\pi\sigma}{i\omega} \quad (2)$$

Ignoring, for the moment only, any dependence of σ on the wave number, its frequency dependence is given by

$$\sigma = \frac{Ne^2\tau}{m^*(1+i\omega\tau)} \quad (3)$$

where τ is the mean time between scattering of the conduction electrons by imperfections or vibrations of the ion-core lattice ($\tau \sim 10^{-14}$ second in metals at room temperature), and N is the conduction-electron density. The magnitude of the conductivity defines a characteristic plasma frequency $\omega_p = (4\pi Ne^2/m^*)^{1/2} \sim 10^{16}$ radians per second at electron densities in metals. For frequencies such that $\omega\tau \gg 1$ the simple expression,

$$\epsilon = \epsilon_l - \frac{\omega_p^2}{\omega^2} \quad (4)$$

displays the inductive shielding of conduction currents (ϵ negative, k imaginary) when $\omega < \omega_p$ and the more usual dielectric behavior for $\omega > \omega_p$. Such a transition from a reflecting to a transmitting state of a plasma is familiar in the case of the ionosphere where broadcastband signals are reflected down to over-the-horizon receivers whereas higher frequency FM and television signals are limited to line-of-sight propagation.

In metals electron scattering becomes important at infrared and lower frequencies ($\omega\tau < 1$) and leads to resistive dissipation as well as inductive shielding. However, the penetration or skin depth $\delta \sim 1/|k|$ remains small ($\delta \sim 10^{-4}$ centimeter at microwave frequencies) and the reflectivity correspondingly high (99.9 percent or better). In order to observe relatively undamped wave propagation in metals at frequencies below the plasma frequency it is necessary to greatly increase the scattering time τ . This can be done by cooling highly purified and unstrained metals to liquid helium temperatures, at which scattering from lattice vibrations, defects, and impurities is minimized. In the case of sodium and potassium the increase in τ amounts to a factor of $\sim 10^4$ in carefully distilled samples (factors as large as 10^6 have been observed in certain other metals).

It might appear that increasing τ would simply extend to lower fre-

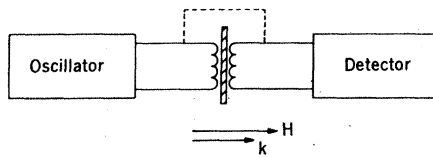


Fig. 2. A highly schematic view of a helicon wave transmission experiment; necessary details such as Dewar vessels have been omitted for clarity. A fraction of the driving signal is used to provide a phase reference (indicated by the dashed connection) for the detector. The magnetic field \mathbf{H} and wave vector \mathbf{k} are applied normal to the plane of the sample.

quencies the region of loss-free total reflection mentioned above. That this is not so results from the changed spatial character of the electron motion. Although at room temperature the mean-free-path between scattering events $\Lambda = v_F\tau$ is ~ 100 angstroms, it becomes ~ 0.1 millimeter in the pure cold metal; and as soon as the mean-free-path becomes appreciably greater than the skin depth the nature of the reflection phenomenon changes subtly. Now electrons moving at large angles with respect to the metal surface participate in the shielding process over only a small fraction of their free path. They are then said to be ineffective. Only the conduction electrons traveling at angles less than δ/Λ with respect to the surface are truly effective over their entire trajectories. Thus, the high frequency skin depth is "anomalous" be-

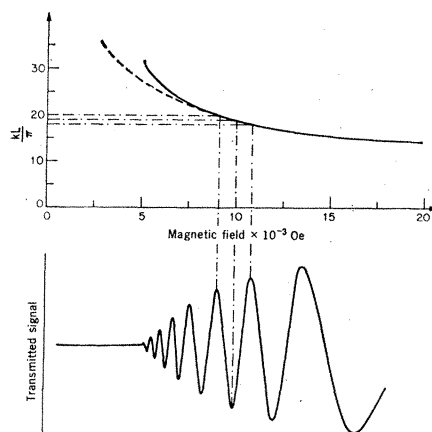


Fig. 3. The upper graph shows the variation of helicon wave number versus magnetic field strength in potassium metal at 200 kilohertz. The solid curve, including corrections for short wavelengths, deviates from the simple $H^{-1/2}$ behavior. Damping due to doppler-shifted cyclotron resonance sets in near 5 kilooersteds. The lower trace shows the corresponding variations in amplitude and phase (with reference to the driving signal) of the signal transmitted through a slab of thickness $L = 1$ millimeter.

cause it does not decrease very much below 100°K as does the d-c resistance of the metal (3). Furthermore, the structure of the damped penetrating wave is changed because the ineffective electrons do carry small amounts of energy deep into the metal.

It is this ability of the long conduction-electron trajectories to transport electromagnetic disturbances over appreciable distances and time intervals which leads to the existence of magnetotransparencies. A magnetic field \mathbf{H} exerts the Lorentz force $e\mathbf{v} \times \mathbf{H}/c$ perpendicular to both \mathbf{H} and to \mathbf{v}_\perp , the transverse component of an electron's velocity. The electron's trajectory is thus curled into a helical cyclotron orbit. The angular frequency of the transverse motion is $\omega_c = eH/m^*c$, the cyclotron frequency, and the radius of gyration is $R_c = v_\perp/\omega_c$. This motion is, of course, well defined only if $\omega_c\tau > 1$ or, correspondingly, $\Lambda > R_c$. Clearly, such cyclotron motion acts to reduce the metal's electrical conductivity transverse to the magnetic field.

In fact the conductivity becomes a rather complicated (tensor) quantity relating current and electric field components which are perpendicular as well as parallel to each other. The conductivity now depends not only on the driving frequency ω in relation to ω_p and τ but also on the direction and strength of the magnetic field, which determines ω_c . Furthermore, σ now depends sensitively on the spatial variation of any electrical disturbance in relation to the orbit radius R_c . With such a wealth of parameters to juggle it is not surprising that novel phenomena are observed!

The Helicon

The simplest, and most familiar of all solid-state plasma waves is a circularly polarized electromagnetic excitation which propagates best along the magnetic flux lines at audio and radio frequencies. Because its electric (or magnetic) field vector traces a spiral path into the metal it is known as the helicon. The theoretical possibility of such a wave was predicted by Konstantinov and Perel (4) and by Aigrain (5) but the helicon was independently discovered experimentally in sodium metal by Bowers, Legendy, and Rose (6). It is closely related to radio-frequency "whistler" modes which travel through the ionosphere along the earth's magnetic flux lines.

A highly idealized experimental arrangement is shown in Fig. 2. An oscillator drives a transmitter coil placed near one face of a plane-parallel sample and induces eddy currents on the sample's surface. A well-shielded receiver coil at the other face picks up a fraction of any energy transmitted along the magnetic field which, in the helicon experiment, is perpendicular to the sample plane. By purposely mixing some of the driving signal with the transmitted component the detector is made sensitive to the phase of the transmitted wave. A variety of other experimental arrangements have been used but this transmitter-receiver scheme is as sensitive as any of them and is conceptually very clear.

The effect of the magnetic field on the dielectric response of the metal in this field-normal geometry is quite simple if one thinks in terms of propagation at wavelengths long compared to the maximal cyclotron radius $R_c = v_F/\omega_c$. Because of their circulation around the flux lines the electrons sense a much different frequency $\omega \pm \omega_c$, depending on the sign of the field. If \mathbf{H} is taken in the sense which turns the electrons in the direction of rotation of the circularly polarized driving currents, the effective dielectric constant becomes

$$\epsilon = \epsilon_l - \frac{\omega_p^2}{\omega[\omega - \omega_c + (i/\tau)]} \quad (5)$$

In the high field limit where ω_c/ω and $\omega_c\tau$ are large and if we neglect ϵ_l (always valid well below the plasma frequency) ϵ further simplifies to

$$\epsilon = \frac{\omega_p^2}{\omega\omega_c} \quad (6)$$

Since ϵ is entirely real the metal has been made transparent. Essentially the electrons "see" a negative frequency and therefore behave as a capacitive rather than an inductive medium.

The variation of $k = k_0(\epsilon)^{1/2}$ with magnetic field is shown in Fig. 3 for the case of potassium driven at 200 kilohertz. The rapidly varying amplitude and phase of the transmitted signal are also sketched. Damping due to finite $\omega_c\tau$ prevents sharpening of the pattern by standing-wave effects though such spatial resonances are observable in some metals.

Beyond its esthetic appeal the experiment measures the ratio $\omega_p^2/\omega_c \propto Ne$, the charge density of the metal. In this sense the helicon is an alternating current version of the Hall effect, capable of high precision due to its spectroscopic character.

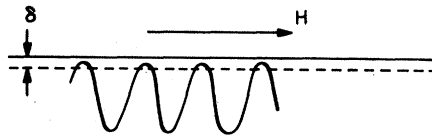


Fig. 4. The Azbel'-Kaner cyclotron resonance geometry. The path of an effective electron is traced. Effective electrons return repeatedly to the skin-effect region where they act to screen the metal when they are in phase with the surface currents.

The long wavelength assumption ($kR_c < 1$) may obviously be fulfilled at sufficiently high magnetic field strengths and, equally obviously, must break down at sufficiently low field strengths. The mathematics then becomes more complicated, but the result is that k increases even more rapidly as the magnetic field decreases (Fig. 3).

Another effect of greater importance intrudes as $kR_c \rightarrow 1$. An electron spiraling around the flux lines is also, in general, traveling very rapidly along them with some fraction $v_{||}$ of the Fermi velocity v_F . It senses the helicon frequency to be doppler-shifted to $\omega_{DS} = kv_{||} \pm \omega$. If the shifted frequency is equal to that of the electron's transverse cyclotron motion the electron is steadily accelerated by the helicon electric field and, in turn, this damps the wave. Since $v_{||}$ may range from $+v_F$ to $-v_F$ and ω is negligibly small compared to ω_c the helicon is cyclotron damped at all wave vectors larger than $kv_F = \omega_c$ (or $kR_c = 1$). The resulting cutoff of the transmission, shown in Fig. 3, provides a measurement of the product m^*v_F , that is, the Fermi momentum p_F . This cyclotron damping effectively confines the study of helicons in metals to the region below 1000 megahertz in presently available magnetic fields.

Cyclotron Waves

Even though the helicon propagates freely in simple metals only at frequencies well above the cyclotron resonance $\omega_c = \omega$, it is clearly the interplay of these two frequencies which dominates the phenomenon. By rotating the magnetic field into the plane of the sample it is possible to observe an entirely new class of plasma waves that are very closely related to the cyclotron resonance and its harmonics, $\omega = \omega_c, 2\omega_c, 3\omega_c$, and so on.

The importance of the field-parallel geometry was first pointed out theoretically by Azbel' and Kaner (7). They

showed that well-defined changes in the anomalous skin-effect dissipation would occur at $\omega = n\omega_c$ because cyclotron motion of the most effective electrons brings them repeatedly back into the surface region (see Fig. 4). At resonance the electrons always return in phase with the driving electric field, and this results in improved shielding of the metal. Such experiments are performed at microwave frequencies, $\omega \approx 10^{11}$ radians per second, to satisfy the requirement that $\omega\tau \gg 1$. Azbel'-Kaner resonances were first observed by Fawcett (8), and since then the experiment has been widely exploited as the most direct and precise means of determining the effective mass of conduction electrons in metals. In sodium and potassium, Grimes and Kip (9) measured $m^*/m_0 = 1.24$ and 1.21, respectively, the mass enhancements resulted from electron-electron and electron-phonon interactions as mentioned earlier.

Going beyond the single-particle aspects of this geometrical configuration Kaner and Skobov analyzed the total dielectric response, seeking wave propagation perpendicular to the magnetic field (10). They found that weakly damped collective excitations should exist near each of the cyclotron resonances with short wavelengths comparable to the anomalous skin depth. However, the first experimentally observed wave propagation near the Azbel'-Kaner resonances was shown to occur with much longer wavelengths, (11). Recently it has become apparent that these cyclotron waves, sometimes known as high-frequency waves to distinguish them from helicons, are at the long wavelength limit of the dispersion curves calculated by Kaner and Skobov (12, 13). Qualitatively similar wave propagation transverse to the magnetic field near the cyclotron resonance and its harmonics occurs in gaseous plasmas where the excitations are known as Bernstein modes (14).

Because the full mathematical treatment is difficult to follow, it may be more useful to illustrate the nature of cyclotron waves with the simplest example. Under long mean-free-path conditions the current at a given point and time in the metal is proportional to the net velocity of the electrons passing through that point. Not only are the electrons accelerated by the electric field at the point itself but they bring with them the effect of electric fields at other points and earlier times, back to their most recent scattering events. If the sum of these local and nonlocal

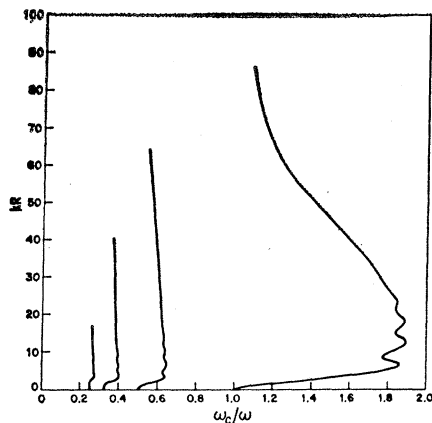


Fig. 5. Cyclotron wave dispersion curves originating at the Azbel-Kaner cyclotron resonances $\omega_c = \omega/n$. The wave number k is normalized to the maximal cyclotron orbit radius R for $\omega_c = \omega$. The large k regions (Kaner-Skobov regime) have not been observed directly but the behavior as $k \rightarrow 0$ has been verified.

contributions can be made to very nearly cancel each other for some combination of k , ω and ω_c the corresponding conductivity becomes vanishingly small and energy propagates. Near the fundamental cyclotron resonance ($\omega_c \approx \omega$) and in the limit of long wavelengths ($kR_c < 1$) the effective dielectric constant for currents polarized parallel to the magnetic field is

$$\epsilon = -\frac{\omega_p^2}{\omega^2} \left[1 + \frac{(kR_c)^2}{5 \left(\frac{\omega^2}{\omega_c^2} - 1 \right)} \right] \quad (7)$$

The second term in the brackets is the nonlocal contribution which, because of its resonant denominator, is able to

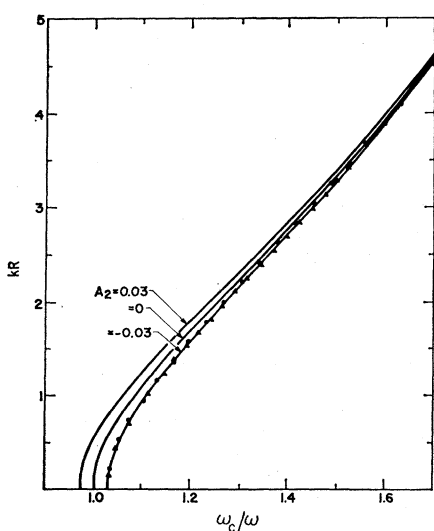


Fig. 6. This expanded view of Fig. 5 illustrates the effect of a finite correlation parameter A_2 on the long wavelength dispersion of the cyclotron wave originating at $\omega_c = \omega$ in the current-parallel-to-field polarization.

cancel the first term, the local contribution, for ω_c just slightly greater than ω .

When this approach is carried out for arbitrary wavelength and all values of the ratio ω_c/ω the result is a series of dispersion curves $k_n(\omega_c/\omega)$, each originating at a cyclotron resonance, $\omega_c = \omega/n$, as shown in Fig. 5. In the terminology of the gas plasma physicist these are the "ordinary" modes. If the driving currents are polarized perpendicular to the magnetic field, similar but more oscillatory dispersion curves are again found to the high-field side of each cyclotron resonance (13) and are called "extraordinary" modes.

Experimentally, most of the long wavelength features of the cyclotron waves at ω_c near ω and $\omega/2$ have been verified in thin plates of potassium (12, 15) and, to a lesser extent, in sodium (16), where lower $\omega\tau$ values complicate the analysis and damp the waves. A minor discrepancy in the intercept of the dispersion curve corresponding to Eq. 7 has been reliably established, however, in both metals. In each case the $k \rightarrow 0$ limit of the curve falls a few percent higher in magnetic field than would be expected from the well-established effective mass values. Although modest in magnitude these deviations prove to be due to the residual (explicit) quasiparticle interactions not properly taken into account in the nearly-free-electron model.

Recently, Henningsen (17) has demonstrated in metallic silver that the large wave number regime of the cyclotron waves ($kR > 1$) is also experimentally accessible in the extraordinary polarization. Preliminary data for potassium (18) confirm the expected oscillatory character of the dispersion curves.

Explicit Many-Body Interactions

In the case of weakly excited states of the degenerate Fermi distribution that act as nearly decoupled quasiparticles of mass m^* the residual interactions are most directly described by a theory originally devised by Landau (19) for liquid He^3 . The extension to charged entities was made by Silin (20). The microscopic justification of the Landau-Silin phenomenological theory (21) and the decomposition of its parameters into electron-electron and electron-phonon contributions (22) are formidable topics which we shall ignore.

It may, however, be of help to draw an analogy between the concept of a

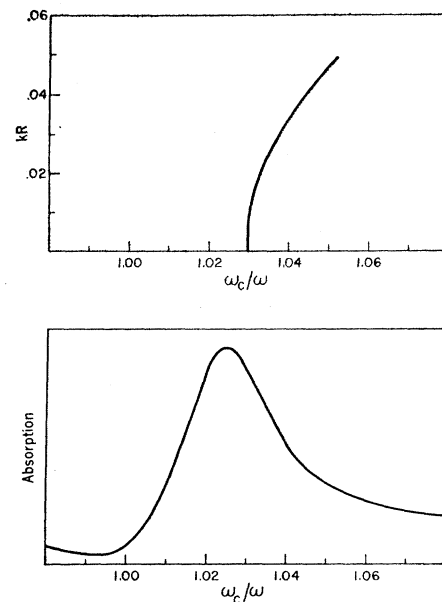


Fig. 7. The upper curve shows correlation-induced dispersion calculated by Cheng, Clarke, and Mermin (24) for $A_2 = -0.03$; $A_1 = 0$, $l \geq 3$; as in potassium. Lower trace shows the absorption experimentally observed by Baraff, Grimes, and Platzman (25).

quasiparticle in the interacting conduction-electron system and the concept of a phonon in a crystal lattice. Rather than treat the complicated and highly correlated mechanical oscillations of the ions or atoms about their equilibrium positions on an individual basis it proves vastly more revealing to speak in terms of lattice waves or normal modes whose frequencies (energies) and wave numbers (momenta) are quantized. These particle-wave entities, the phonons, are completely decoupled from one another if the binding forces on the ions are harmonic. They may also scatter off of each other, while total energy and momentum are conserved, if the forces are somewhat anharmonic. In the case of the coupled electron fluid or Fermi liquid the analogous collective entities are the quasiparticles. They are never completely decoupled, however, and the object of the Landau-Silin theory is the description of the residual interactions.

From the experimental viewpoint it is sufficient that quasiparticles are weakly coupled via a two-body scattering function $f(\mathbf{p}, \mathbf{S}; \mathbf{p}', \mathbf{S}')$. In the absence of appreciable spin-orbit coupling f may be divided into a spin-independent correlation component $f^s(\mathbf{p}, \mathbf{p}')$, which influences only electrical phenomena, and a spin-dependent part $f^a(\mathbf{p}, \mathbf{p}') \mathbf{S} \cdot \mathbf{S}'$. The latter exchange coupling affects magnetic properties. In an isotropic system the magnitudes of \mathbf{p}

and \mathbf{p}' are essentially the Fermi momentum p_F . The functions f^s and f^a may therefore be expanded in a Legendre polynomial series in $\hat{\mathbf{p}} \cdot \hat{\mathbf{p}}' = \cos \theta$:

$$f^s = \sum_{l=0}^{\infty} A_l \rho_l P_l(\cos \theta) \quad (8)$$

$$f^a = \sum_{l=0}^{\infty} B_l \rho_l P_l(\cos \theta) \quad (9)$$

where the $\rho_l = \pi^2(2l+1)/m^*p_F$ serve to make the coefficients A_l and B_l dimensionless. The sets of electric and magnetic coefficients are the Fermi-liquid parameters which, together with m^* , completely describe the excitations near the Fermi energy of the electron fluid.

It is possible to argue rather generally that the electric coefficients, A_l , should be expected to significantly influence transport properties only if kv_F , ω , and ω_c are all roughly comparable. This is exactly the situation in the case of the cyclotron waves but is not practically attainable for helicons. As if to compensate for this the correlations actually introduce new modes in the field-normal geometry near $\omega = \omega_c$, well below the cyclotron damping frequency of the helicon. These will be briefly discussed later.

The effects of nonvanishing A_l on the cyclotron waves are most easily evaluated in the long wavelength limit. In principle each of the cyclotron resonances becomes a set of discrete singularities at $\omega = \omega_{ln} = n\omega_c(1 + A_l)$. In present practice neither A_0 nor A_1 measurably affect the plasma waves. A_0 influences only charge separations, which are always negligible for $\omega \ll \omega_p$. A_1 influences only finite current flow whereas, at long wavelengths, the cyclotron waves correspond almost exactly to zeroes of the microwave conductivity. Finally at A_2 and the higher order A_l observable effects are possible because these coefficients couple the more complicated electron velocity changes.

The effect of A_2 is to shift the long wavelength intercept of the mode of Eq. 7 from $\omega = \omega_c$ to $\omega = \omega_c(1 + A_2)$. The excellent fit to the experimental dispersion data for potassium (Fig. 6) was calculated for $A_2 = -0.03$, $A_l = 0$ for all $l \geq 3$ (23). A similar analysis yields $A_2 = -0.05$ in sodium. The higher order parameters appear to be quite small, $|A_3| < 0.01$, in both metals. No evidence for new modes originating at the predicted extra singularities has been observed. This is not

too surprising because the coupling to modes entirely dependent on correlation effects for their existence is expected to be extremely weak and therefore very difficult to discern against the background of nearly-free-electron modes and the single-particle Azbel'-Kaner resonances.

Correlation Dependent Modes

The possibility of detecting weakly coupled modes becomes significantly greater if one returns to the field-normal geometry. Cheng, Clarke, and Mermin (24) find that, in this case, correlations do indeed introduce new long wavelength modes slightly shifted from $\omega = \omega_c$, a region where no other phe-

nomena are expected to occur. For the case $A_2 = -0.03$ (all higher $A_l = 0$) appropriate to potassium they predict a new transparency whose $k=0$ intercept lies at $\omega_c = \omega/(1 + A_2)$ and which becomes severely cyclotron damped at $\omega_c = \omega[(1 + 5A_2)/(1 + A_2)]$ as shown in Fig. 7. Although no clear-cut interference pattern has been observed, Baraff, Grimes, and Platzman (25) have found a well-defined absorption peak in potassium in the appropriate field range. This appears to only be attributable to increased penetration of microwaves into the metal surface due to the correlation-dependent mode. No evidence has been found for other modes which should exist in this region if the higher order A_l were of significant magnitude.

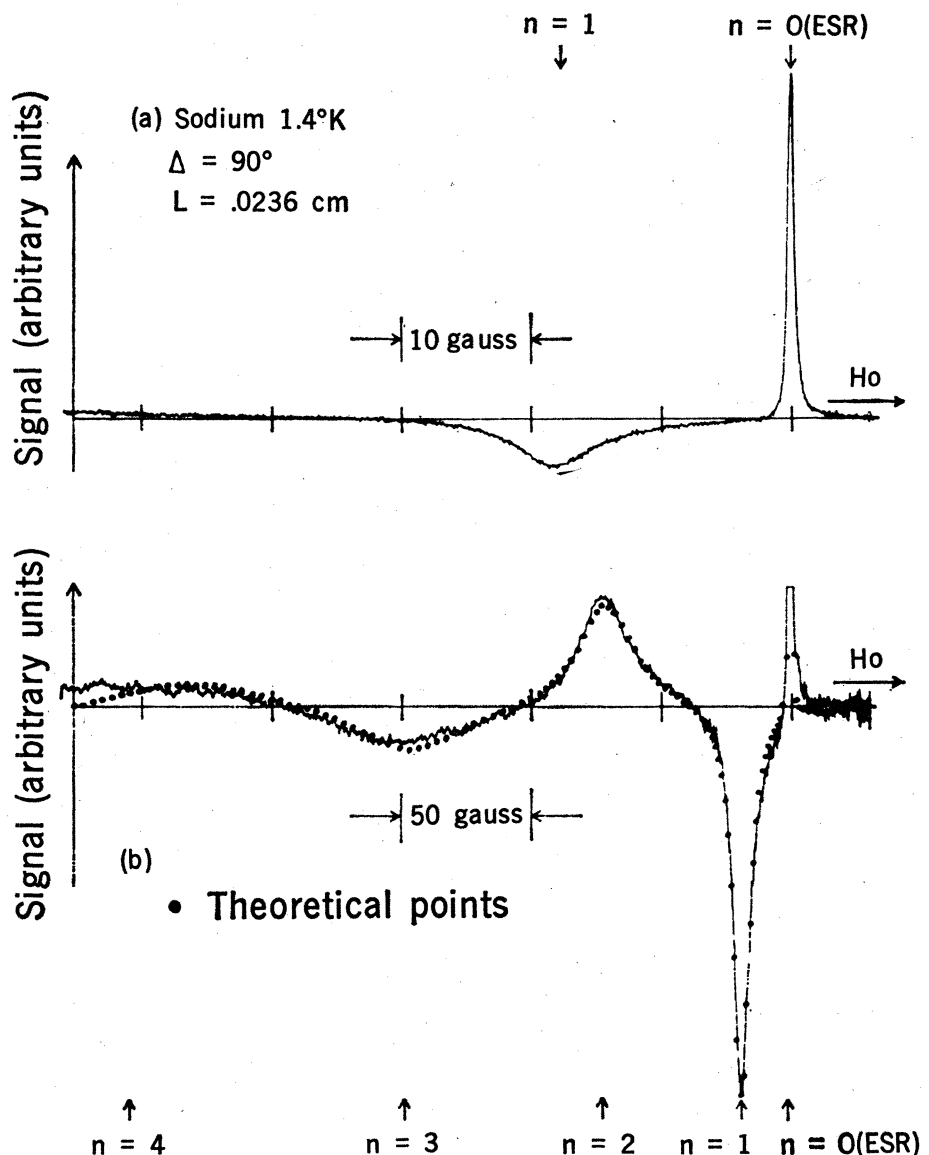


Fig. 8. Microwave transmission through sodium metal by diffusion of resonant conduction electrons and excitation of standing spin waves [after Schultz and Dunifer (26)]. The upper trace shows the intense narrow CESR line due to the uniform precession mode ($n=0$) and the first sideband due to nonuniform precession of wavelength $\lambda = 2L$, $n=1$. The lower trace shows the first four sidebands and a comparison with theoretical points computed using the theory of Platzman and Wolff (27).

Paramagnetic Spin Waves

By ignoring the historical order of events the most striking evidence of wave propagation entirely due to many-body interactions has been left until the end of the story. While examining the microwave transmission occurring at conduction electron spin resonance (CESR) Schultz and Dunifer (26) discovered a series of extra transmission peaks of alternating phase. These lay to the low-field side of the resonance in the field-parallel geometry and moved to the high-field side when the magnet was rotated normal to the plate. Platzman and Wolff (27) attributed this phenomenon to standing spin waves that resulted from exchange coupling between the quasiparticle spins described by the antisymmetric interaction function $f^a(\mathbf{p}, \mathbf{p}') \mathbf{S} \cdot \mathbf{S}'$.

The presence of a magnetic field causes the small number of unpaired spin magnetic moments in the vicinity of the Fermi level to precess at the angular frequency $\omega_s = g\beta H$ where $\beta = eH/2m_0c$ is the Bohr magneton. The g factor in the light alkali metals is quite close to the free-electron value 2.0023 because their spin-orbit couplings are very weak. Such decoupling is essential in the separation of the interaction function f into independent correlation and exchange contributions. The weak spin-orbit coupling also leads to a spin precession lifetime T_1 very much longer than the orbital collision time τ . Thus even at room temperature the nonequilibrium magnetization created in the skin-effect region of a metal at $\omega = \omega_s$ (analogous to paramagnetic resonance of localized unpaired magnetic moments in insulators) is carried deep within the metal. In this manner electromagnetic energy may be transported in the spin system to be radiated at the far surface of an appropriate slab. The characteristic "spin depth" $\delta_s = v_F(2T_1\tau/3)^{1/2}$ is the result of a random walk or diffusion of T_1/τ steps during the decay time T_1 .

At low temperatures this process becomes anisotropic as τ becomes larger, and the orbital motion in the magnetic field is curled into the helical cyclotron orbits. If, in addition, exchange forces tend to align adjacent spin magnetic moments the transport of magnetization loses its diffuse character and becomes a wavelike process with a well-defined wave number determined by the interplay of spin precession and cyclotron transport. There is only a qualitative analogy between these very

weak spin waves and the more familiar ferromagnetic spin waves which are more readily observed in strongly ferromagnetic metals such as nickel and iron where large exchange forces dominate the entire behavior of the unpaired electrons.

Because the magnetization is so small in the alkali metals the complete boundary value problem can be solved accurately; this is evident in Fig. 8 where the experimental and theoretical transmission spectra for sodium are compared. The response of the spin system is given by the generalized magnetic susceptibility

$$\chi(k, \omega, \omega_s) = \chi_{\text{static}} \frac{\omega_s}{\omega_s - \omega - (i/T_1') - ik^2 D} \quad (10)$$

analogous to the generalized electrical conductivity discussed earlier. In the limit $k \rightarrow 0$, χ is resonant at $\omega = \omega_s$ in the usual CESR fashion but also has a wave-number dependent spin-wave character given by $\omega_s - \omega - ik^2 D = 0$. The "diffusion constant"

$$D = \frac{v_F^2 \tau}{3} (1 + B_0) (1 + B_1) \times \left(\frac{\cos^2 \Delta}{X^2} + \frac{\sin^2 \Delta}{X^2 + \omega_c^2 \tau^2} \right) \quad (11)$$

where

$$X = 1 - i \left(\frac{B_0 - B_1}{1 + B_0} \right) \omega_s \tau \quad (12)$$

contains both the anisotropic influence of cyclotron motion via the angle Δ between \mathbf{k} and \mathbf{H} and the exchange coupling via the two lowest-order magnetic Fermi-liquid parameters B_0 and B_1 . Careful measurements of the angular dependence of the spin-wave peaks and of the sample thickness yield values of $B_0 = -0.18$ and $B_1 = 0.05$ for sodium, $B_0 = -0.26$ and $B_1 = -0.01$ for potassium (28).

Two other effects of the exchange interaction are also inherent in Eq. 10. Both the static Pauli susceptibility and the spin lifetime T_1' are enhanced over their free-electron values by the lowest order parameter B_0 :

$$\chi_{\text{static}} = \chi_0 m^*/m(1 + B_0)$$

and

$$T_1' = T_1/(1 + B_0)$$

In the case of χ_{static} it is possible to deduce B_0 from a careful magnetization experiment; but the spin waves are likely, because of their spectroscopic character, to prove a more accurate probe.

Conclusion

A wealth of new phenomena and of quantitative information, much of it unobtainable by other means, has been provided by studies of wave propagation in the conduction-electron plasmas of sodium and potassium. It appears to be generally true that "where there are resonances there are waves." The direct experimental observation of explicit many-body effects has had particular interest for the study of the fundamental properties of the interacting electron fluid. Similar investigations will prove rewarding in the heavier alkalis and even in metals where band structure effects play a dominant role. However, analysis of these cases will be much more difficult in practice if not in principle.

References and Notes

1. T. H. Stix, *The Theory of Plasma Waves* (McGraw-Hill, New York, 1962).
2. *Symposium on Plasma Effects in Solids, 1964* (Academic Press, New York, 1965).
3. A. B. Pippard, *Advan. Electron. Electron Phys.* **6**, 1 (1954).
4. O. V. Konstantinov and V. I. Perel, *Zh. Eksp. Teor. Fiz.* **38**, 161 (1960) [translated in *Sov. Phys. JETP* **11**, 117 (1960)].
5. P. Aigrain, *Proceedings of the International Conference on Semiconductor Physics, Prague, 1960* (Czechoslovak Academy of Sciences, Prague, 1961).
6. R. Bowers, C. Legendy, F. Rose, *Phys. Rev. Lett.* **7**, 339 (1961).
7. M. Ya. Azbel' and E. A. Kaner, *Zh. Eksp. Teor. Fiz.* **30**, 811 (1956) [translated in *Sov. Phys. JETP* **3**, 772 (1956)].
8. E. Fawcett, *Phys. Rev.* **103**, 1582 (1956).
9. C. C. Grimes and A. F. Kip, *ibid.* **132**, 1991 (1962).
10. E. A. Kaner and V. G. Skobov, *Fiz. Tverd. Tela* **6**, 1104 (1964) [translated in *Sov. Phys. Solid State* **6**, 51 (1964)].
11. W. M. Walsh, Jr., and P. M. Platzman, *Phys. Rev. Lett.* **15**, 784 (1965).
12. P. M. Platzman, W. M. Walsh, Jr., E-Ni Foo, *Phys. Rev.* **172**, 689 (1968).
13. E-Ni Foo, *ibid.* **182**, 674 (1969).
14. I. B. Bernstein, *ibid.* **109**, 10 (1958).
15. W. M. Walsh, Jr., P. M. Platzman, P. S. Peercy, L. W. Rupp, Jr., P. H. Schmidt, *Proceedings of the Conference on Low Temperature Physics, 12, Kyoto 1970*, in press.
16. W. M. Walsh, Jr., in *Electrons in Metals, Proceedings of the Simon Fraser Summer School*, J. F. Cochran and R. R. Haering, Eds. (Gordon and Breach, New York, 1968); S. Schultz and D. R. Fredkin (unpublished).
17. J. O. Henningsen, *Phys. Rev. Lett.* **24**, 823 (1970).
18. G. Dunifer, personal communication.
19. L. D. Landau, *Zh. Eksp. Teor. Fiz.* **30**, 1058 (1956) [translated in *Sov. Phys. JETP* **3**, 920 (1956)].
20. V. P. Silin, *ibid.* **33**, 495 (1957) [translated in *Sov. Phys. JETP* **6**, 945 (1958)].
21. P. Nozières, *The Theory of Interacting Fermi Systems* (Benjamin, New York, 1964).
22. T. M. Rice, *Phys. Rev.* **175**, 858 (1968).
23. E-Ni Foo, unpublished result.
24. Y. C. Cheng, J. S. Clarke, N. D. Mermin, *Phys. Rev. Lett.* **20**, 1486 (1968).
25. G. A. Baraff, C. C. Grimes, P. M. Platzman, *ibid.* **22**, 590 (1969).
26. S. Schultz and G. Dunifer, *ibid.* **18**, 283 (1967).
27. P. M. Platzman and P. A. Wolff, *ibid.*, p. 280.
28. S. Schultz and G. Dunifer, unpublished result.
29. I wish to thank my colleagues, Drs. G. A. Baraff, G. L. Dunifer, C. C. Grimes, P. M. Platzman, and T. M. Rice, for many helpful conversations.